




# Isomerization of $\alpha$ -pinene oxide to campholenic aldehyde in the presence of Al-SiO<sub>2</sub> and magnetic Al-SiO<sub>2</sub>/Fe<sub>3</sub>O<sub>4</sub> catalysts

V. N. Panchenko<sup>1,2</sup> · V. L. Kirillov<sup>1</sup> · E. Yu. Gerasimov<sup>1</sup> · O. N. Martyanov<sup>1</sup> · M. N. Timofeeva<sup>1,2</sup> 

Received: 18 March 2020 / Accepted: 13 June 2020 / Published online: 8 July 2020  
© Akadémiai Kiadó, Budapest, Hungary 2020

## Abstract

In the present work, we demonstrated synthesis of Al-SiO<sub>2</sub> and magnetically recoverable Al-SiO<sub>2</sub>/Fe<sub>3</sub>O<sub>4</sub> systems via grafting of triethylaluminum on SiO<sub>2</sub> and SiO<sub>2</sub>-coated magnetic Fe<sub>3</sub>O<sub>4</sub> nanoparticles, respectively. These materials were characterized by various techniques including elemental and N<sub>2</sub>-adsorption/desorption analyses, transmission electron microscopy (TEM), and Fourier transform infrared spectroscopy (FTIR) using CO and pyridine as probe molecules. Amount of grafted Al on the support was found to affect the textural, acid–base properties and catalytic behavior in the isomerization of  $\alpha$ -pinene oxide (PO) to campholenic aldehyde (CA). Maximal activity and selectivity towards CA was observed in the presence of sample with 12 wt% of alumina. It was demonstrated that 12% Al-SiO<sub>2</sub>/Fe<sub>3</sub>O<sub>4</sub> can be used as catalyst for at least four successive cycles without loss of activity.

**Keywords** Isomerization ·  $\alpha$ -Pinene oxide · Campholenic aldehyde · Magnetic nanoparticle · Al-containing silica · Lewis acidity

---

**Electronic supplementary material** The online version of this article (<https://doi.org/10.1007/s11144-020-01811-x>) contains supplementary material, which is available to authorized users.

---

✉ M. N. Timofeeva  
timofeeva@catalysis.ru

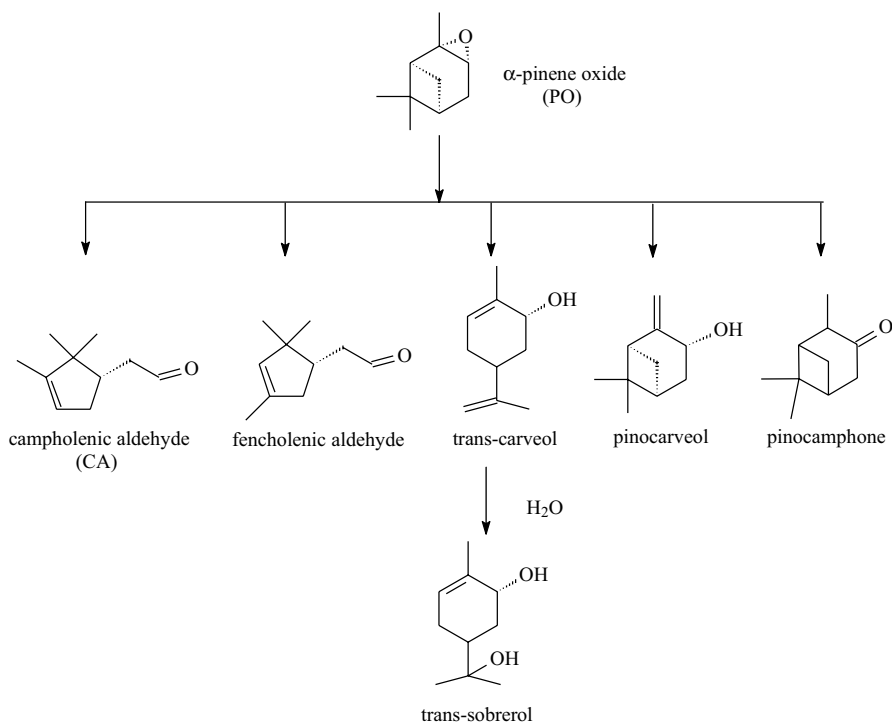
<sup>1</sup> Borekov Institute of Catalysis SB RAS, Prospekt Akad. Lavrentieva 5, Novosibirsk, Russian Federation 630090

<sup>2</sup> Novosibirsk State Technical University, Prospekt K. Marksa 20, Novosibirsk, Russian Federation 630092

## Introduction

Terpenes and their epoxides are widely used as precursors for the synthesis of fragrances, flavors and pharmaceuticals [1]. In particular,  $\alpha$ -pinene oxide (PO) can be converted by acid-catalyzed transformations in ca. 200 substances [2] which can be applied in the fine chemicals industry. Campholenic aldehyde (CA), *trans*-carveol (*trans*-carv) and *trans*-sobrerol (*trans*-sobr) are the most important compound among of this diversity (Scheme 1). Thus, CA is utilized as an intermediate for the production of sandalwood fragrances [3] and as an environmental friendly substitute for nitro and polycyclic musks in laundry detergents and softeners [4].

Isomerization of PO to CA mainly proceeds in the presence of systems with Lewis acid sites (LAS), while systems having Brønsted acid sites (BAS) favor to form *trans*-carveol and *trans*-sobrerol [5–7]. In the presence of Brønsted type catalytic systems selectivity towards CA is 50–60%, while Lewis acids, for example, industrial catalyst  $\text{ZnCl}_2$ , give selectivity up to 80–85% [7]. Note that  $\text{ZnCl}_2$  application has several disadvantages, such as lack of regeneration, corrosion problems, toxicity, and waste water pollution. Nowadays, the replacement of the homogeneous catalyst by new heterogeneous catalyst is a challenging goal of the fine chemicals industry.

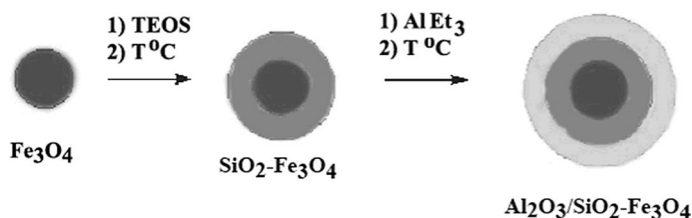


**Scheme 1** Products obtained in the course of PO rearrangement

Currently, considerable attention is focused on the development of new solid Lewis catalysts [7–13] with the main effort being on composite materials with micro-/mesoporous structure. Such type materials improve mass transfer and accessibility of active sites that allow to reduce steric and diffusional limitations, and formation of by-products in catalytic reactions. Thus, a 70% selectivity at a lower conversion of PO (18%) were observed in the presence of microporous 15%Al<sub>2</sub>O<sub>3</sub>-SiO<sub>2</sub> at 253 K [14]. According to Holderich et al. [7], the dealumination H-US-Y zeolite by HCl allows to produce CA with 70–80% selectivity due to its unique structure (i.e. a three-dimensional large pore system (7.4 Å) with supercages of 12 Å and many mesopores that make USY zeolites). Note that the performance of H-USY zeolite strongly depends on the SiO<sub>2</sub>/Al<sub>2</sub>O<sub>3</sub> ratio. The selectivity towards CA was about 70% at 398 K after 2 h, when this ratio was 70. Selectivity was improved to about 80% at lower temperatures down to 243 K.

The effect of structure was demonstrated for Al-MSU-S<sub>FAU</sub> (Si/Al 70) having a mesoporous structure with microporous walls [8]. The high selectivity towards CA was explained by the isomerization of PO within the microporous channels. The short length of the channels favors the rapid movement of the reaction products away from the active site that prevents the further reaction to other isomers occurs. The selectivity towards CA was 86% at 54% conversion of PO. It has been stated in the literature that amount of Al in Al,Si-containing materials also can affect the reaction rate and distribution of products. Thus, Liebens et al. [11] demonstrated that the increasing molar ratio of Si/Al from 10.4 to 60% in HY zeolite framework led to the decreasing conversion of PO from 96 to 49% and increasing selectivity towards CA increased from 49 to 66%. The yield of CA decreased from 72 to 13% after changing of Si/Al molar ratio from 70 to 6 in framework of Al<sub>2</sub>O<sub>3</sub>-SiO<sub>2</sub> [15].

The magnetic nanoparticles (MNPs) as the carriers for the synthesis of various catalytic systems for many organic transformations are of considerable recent interest [16–19]. There are several reasons. First of all, the nanoparticles possess a large surface area, which favors the formation of quite an amount of active and accessible centers. Moreover, MNPs allows to simplify separation and filtration and, therefore, to reduce the loss of catalysts in repeated trials. Herein, we wish to demonstrate catalytic properties of the magnetically recyclable Al-SiO<sub>2</sub>/Fe<sub>3</sub>O<sub>4</sub> samples prepared by a post-synthesis grafting method (Scheme 2), which allows to control amount of Al on the surface of solids and, therefore, textural properties and surface acidity [20]. Al-grafting method was successfully used for the design of catalytic systems based on MCM-41 with Si/Al ratios from 15 to 200 mol/mol for synthesis of bisphenol F



**Scheme 2** Synthesis of Al-SiO<sub>2</sub>/Fe<sub>3</sub>O<sub>4</sub> samples

from phenol and formaldehyde [21]. Sample with a Si/Al ratio of 70 mol/mol had the highest activity among of Al-MCM-41 samples that was explained by the effect of Al content in MCM-41 on the amount of acid sites. According to the temperature-programmed desorption of ammonia (NH<sub>3</sub>-TPD), amount of acid sites with weak and medium strength (desorption temperature at 423–673 K) increases with increasing Al content in samples, whereas amount of strong acid sites (desorption temperature at 673–1023 K) is very small and remains constant. We also investigated the effect of Al amount on the textural properties and surface acidity for providing an opportunity to streamline the procedures of Al-SiO<sub>2</sub>/Fe<sub>3</sub>O<sub>4</sub> preparation. For this aim we used the Al-containing silica (Al-SiO<sub>2</sub>) with different Al content prepared by a grafting method. In general, the main purpose of our study was the establishment of correlations between amount of Al, aggregation state of Al, nature of acid sites and catalytic behavior of these materials in isomerization of PO to CA. Analysis of main factors affected the reaction rate and isomer selectivity was performed by combination of spectroscopic and catalytic methods.

## Experimental

### Materials

$\alpha$ -Pinene oxide (95.0%) was purchased from Acros Organics, and SiO<sub>2</sub> was purchased from Davison 752 (Fe content was 0.04 wt%). Commercial dichloroethane (0.1 wt% of water), octane, triethylaluminum (TEA) were used without purification. The following reagents of chemical grade purity were used: 23.5% ammonia aqueous solution (Sigma-Aldrich,  $\geq 99.99\%$ ), FeCl<sub>2</sub>•4H<sub>2</sub>O (Sigma-Aldrich,  $> 99.0\%$ ) and FeCl<sub>3</sub>•6H<sub>2</sub>O (Sigma-Aldrich,  $\geq 98\%$ ).

### Synthesis of Al-SiO<sub>2</sub> samples

Al-SiO<sub>2</sub> samples were synthesised according to Scheme S1 (Supporting Information (SI)). SiO<sub>2</sub> was calcined at 973 K for 6 h in air and cooled in an inert atmosphere (N<sub>2</sub>). Then, a measured amount of 0.329 M TEA in hexane (0.6–20.7 mmol of TEA per 1 g of SiO<sub>2</sub>) was added to SiO<sub>2</sub> and stirred for 2 h at room temperature in a N<sub>2</sub> atmosphere. Al-SiO<sub>2</sub> samples were air dried and then calcined at 973 K for 4 h. The designation of the samples and the conditions of their synthesis are presented in Table 1.

### Synthesis of magnetic Al-SiO<sub>2</sub>/Fe<sub>3</sub>O<sub>4</sub> samples

Al-SiO<sub>2</sub>/Fe<sub>3</sub>O<sub>4</sub> samples were synthesized according to Scheme 2, which shows the synthesis of magnetic Fe<sub>3</sub>O<sub>4</sub> nanoparticles, SiO<sub>2</sub>/Fe<sub>3</sub>O<sub>4</sub> nanoparticles and Al-SiO<sub>2</sub>/Fe<sub>3</sub>O<sub>4</sub> samples. Magnetic Fe<sub>3</sub>O<sub>4</sub> nanoparticles were synthesized was performed according to the procedure reported previously [22]. Magnetic particles were synthesized by co-precipitating Fe<sup>2+</sup> and Fe<sup>3+</sup> salts ([Fe<sup>3+</sup>]/[Fe<sup>2+</sup>]=2). The total concentration of Fe<sup>2+</sup> and Fe<sup>3+</sup> ions was 0.15 M. We performed the synthesis under an

**Table 1** Chemical composition and textural data of Al-SiO<sub>2</sub> and 12%Al-SiO<sub>2</sub>/Fe<sub>3</sub>O<sub>4</sub> materials

Samples	TEA/SiO <sub>2</sub> <sup>b</sup> (mmol/g SiO <sub>2</sub> )	Al content in sample (wt%)	Textural data				
			S <sub>BET</sub> <sup>b</sup> (m <sup>2</sup> /g)	V <sub>Σ</sub> <sup>c</sup> (cm <sup>3</sup> /g)	V <sub>μ</sub> <sup>d</sup> (cm <sup>3</sup> /g)	V <sub>μ</sub> / V <sub>Σ</sub>	D <sub>pore</sub> <sup>d</sup> (nm)
SiO <sub>2</sub>	–	–	225	1.74	0.0	0	21.0
0.5%Al-SiO <sub>2</sub>	0.6	0.5 ± 0.04	219	1.99	0.005	0.003	22.0
1%Al-SiO <sub>2</sub>	1.2	1.0 ± 0.09	200	1.01	0.01	0.010	20.1
4%Al-SiO <sub>2</sub>	4.5	4.0 ± 0.21	225	1.27	0.02	0.016	22.4
6%Al-SiO <sub>2</sub>	6.9	6.0 ± 0.16	267	1.08	0.02	0.019	22.6
12%Al-SiO <sub>2</sub>	13.8	12.0 ± 0.32	303	1.16	0.07	0.060	15.5
18%Al-SiO <sub>2</sub>	20.7	18.0 ± 0.36	223	1.06	0.04	0.038	12.6
SiO <sub>2</sub> /Fe <sub>3</sub> O <sub>4</sub>	–	–	45	0.30	0.0	0	43.6
12%Al-SiO <sub>2</sub> / Fe <sub>3</sub> O <sub>4</sub>	15.0	12.0 ± 0.45	24	0.26	0.02	0.077	36.1

<sup>a</sup>Ratio of TEA/SiO<sub>2</sub> in preparation mixture

<sup>b</sup>S<sub>BET</sub> specific surface area

<sup>c</sup>V<sub>Σ</sub> Total pore volume

<sup>d</sup>Microporous pore volume

<sup>e</sup>D<sub>pore</sub> diameter of pore

Ar atmosphere at room temperature (298 K) by mixing the Fe<sup>2+</sup> and Fe<sup>3+</sup> solution under intense mechanical stirring (500 rpm) with a solution of ammonium hydroxide in deoxygenated water (pH of solution was 11.6). Magnetic Fe<sub>3</sub>O<sub>4</sub> nanoparticles were aged for 3 days in mother liquor at room temperature, then washed with ethanol and used in the next stage of synthesis. TEOS was added to the ethanol solution of magnetic Fe<sub>3</sub>O<sub>4</sub> nanoparticles with size 13.5 nm (0.5 wt%). The amount of TEOS (6.1 mg of TEOS per 1 mg of Fe<sub>3</sub>O<sub>4</sub>) was estimated to give a 5 nm SiO<sub>2</sub> shell on the magnetic nanoparticles. After dispersion by sonication (44 kHz, 60 W, steel emitter within the mixture) for 1 min, the mixture was hydrolyzed by 23% NH<sub>4</sub>OH. Then, this mixture was dispersed by sonication for 1 h and stored for 18 h. The resulting SiO<sub>2</sub>/Fe<sub>3</sub>O<sub>4</sub> was separated from a small amount of solid nonmagnetic parts (~1.5 wt% SiO<sub>2</sub>), washed with ethanol, and dried at room temperature.

The magnetic SiO<sub>2</sub>/Fe<sub>3</sub>O<sub>4</sub> nanoparticles were calcined at 973 K for 6 h in air and cooled in an inert atmosphere (N<sub>2</sub>). Then, a measured amount of 0.329 M TEA in hexane was added to SiO<sub>2</sub>/Fe<sub>3</sub>O<sub>4</sub> and stirred for 2 h at room temperature in an N<sub>2</sub> atmosphere. Al-SiO<sub>2</sub>/Fe<sub>3</sub>O<sub>4</sub> samples were air dried and then calcined at 973 K for 4 h. The synthesis reaction conditions of the Al-SiO<sub>2</sub>/Fe<sub>3</sub>O<sub>4</sub> samples were similar to that of the Al-SiO<sub>2</sub> samples.

## Instrumental measurements

The porous structure of the materials was determined from the adsorption isotherm of N<sub>2</sub> at 80 K on a Micromeritics ASAP 2400. The specific surface area (S<sub>BET</sub>) was

calculated from the adsorption data over the relative pressure range between 0.05 and 0.20. The total pore volume ( $V_{\text{total}}$ ) was calculated from the amount of nitrogen adsorbed at a relative pressure of 0.99.

High-resolution transmission electron microscopy (HR TEM) images were obtained with a JEOL JEM-2010 microscope with a resolution of 1.4 Å operated at an accelerating voltage of 200 kV. The size distribution of the nanoparticles was calculated based on a representative set of HR TEM images taken at different areas of the sample. The number of measured particles was 546. The Al content in Al-containing samples was carried out by means of inductively coupled plasma-atomic emission spectrometry (ICP-AES) using a PERKIN-ELMER instrument OPTIMA 4300.

The nature of functional groups was studied by IR spectroscopy using probe molecules. Analysis of the Lewis surface acidity by CO adsorption of the Al-SiO<sub>2</sub> samples was carried out at 80 K under CO pressure from 13.3 to 1333 Pa. The concentration of Lewis acid sites was estimated from the integral intensity of CO bands in the region above 2180 cm<sup>-1</sup> according to [23] (SI, Sect. 2 “IR spectroscopy study of the acid–base properties of the supports”). Brønsted acidity was investigated by pyridine adsorption according to [23]. The IR spectra were recorded on a FTIR-8400S (Shimadzu) spectrometer with DRS-800 diffusion reflection attachment in the region of 700–6000 cm<sup>-1</sup> with a resolution of 4 cm<sup>-1</sup> using of 100 scans.

## Catalytic test

The isomerization of PO was carried out at 303 K in a glass reactor equipped with a magnetic stirrer. Dichloroethane was used as the solvent. Prior to the reaction, all catalysts were activated at 423 K for 4 h in order to remove any adsorbed water. Then, 0.25 mmol PO, 2 mL of C<sub>2</sub>H<sub>4</sub>Cl<sub>2</sub>, and 10 mmol octane (internal standard), 5 mg of the catalyst were added to the reactor. At different time intervals aliquots were taken from reaction mixture and analyzed. A mass-spectrometer (Shimadzu GCMS QP-2010 Ultra with column GsBP1-MS 30 m × 0.32 mm, thickness 0.25 μm) was used for identify the reaction products. A gas chromatograph (Agilent 7820) with a flame ionization detector on capillary column HP-5 was used to analyze reaction products. The experiment reproducibility was 2–3%.

## Results and discussion

### Optimization of Al-grafting method

#### Effect of Al content on properties of Al-SiO<sub>2</sub> systems

Process of TEA grafting onto SiO<sub>2</sub> was monitored by DRIFT spectroscopy. Fig. 1 shows the DRIFT spectra of SiO<sub>2</sub> activated at 973 K and Al-SiO<sub>2</sub> samples in the Si–OH stretching region. Two bands are observed in all spectra. There are a narrow band at 3745 cm<sup>-1</sup> attributed to the stretching vibration of isolated Si–OH groups

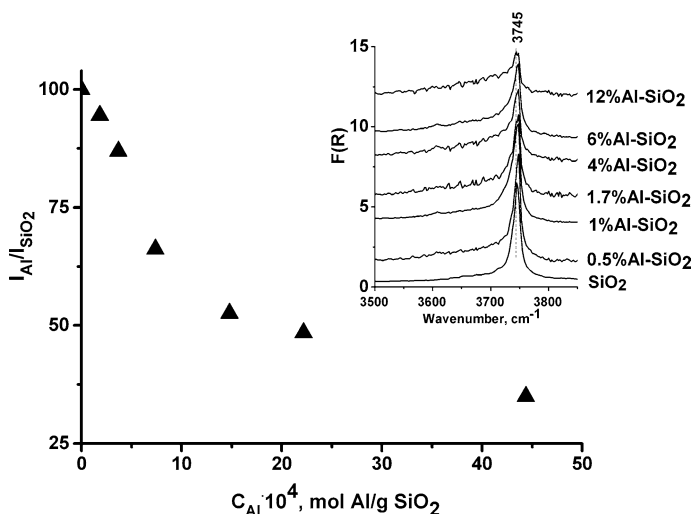


**Fig. 1** Correlation between Al content in Al-SiO<sub>2</sub> and relative intensity of stretching vibrations of terminal of Si–OH groups ( $\nu_{\text{OH}}=3745\text{ cm}^{-1}$ ). ( $I_{\text{Al}}/I_{\text{SiO}_2}$  ratio was calculated from DRIFT spectra of SiO<sub>2</sub> and Al-SiO<sub>2</sub> samples)

and a broad and weak band in the range of 3700–3500  $\text{cm}^{-1}$  assigned to the hydrogen-bonded –OH groups formed due to the interaction Al–OH and Si–OH groups [24–26]. The intensity of band at 3745  $\text{cm}^{-1}$  decreased with increasing Al content in Al-SiO<sub>2</sub> samples (Fig. 1) that can be explained by the interaction between Si–OH groups and TEA. According to Ref. [27], silica dehydroxylated at 973 K contains 2.3  $\mu\text{mol}$  Si–OH per  $\text{m}^2$  of SiO<sub>2</sub>. Based on this, we can say that monolayer coverage of silica by TEA is observed in samples with Al content less than 4–6 wt%. This assertion is consistent with investigation of Iengo et al. [20]. They demonstrated that 2.1 mmol of grafted aluminum alkoxide Al(OR)<sub>3</sub> on 1 g of SiO<sub>2</sub> with a specific surface area of 280  $\text{m}^2/\text{g}$  corresponded to a monolayer coverage, i.e. the Al density was 7.5  $\mu\text{mol Al}/\text{m}^2$ . In our case, the aluminum monolayer coverage was 1.8 mmol/g (about 5 wt%). The subsequent increases in Al content should lead to the polylayer coverage of the SiO<sub>2</sub> surface (i.e. the formation of Al<sub>2</sub>O<sub>3</sub> agglomerates). This suggestion agrees with the change in textural properties of Al-SiO<sub>2</sub> samples. One can be seen from Table 1, specific surface area and microporosity of samples raised with increasing Al content up to 12 wt% and then decreased dramatically, that can be related to the impact of Al on the Al<sub>2</sub>O<sub>3</sub> oligomeric state on the surface of Al-SiO<sub>2</sub>.

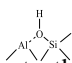
The drastic changes of the nature and amount of –OH groups should undoubtedly affect the surface acidity of Al-SiO<sub>2</sub> samples. The changes in the surface acidity of Al-SiO<sub>2</sub> samples were investigated by FTIR spectroscopy. Pyridine and CO were used as the probe molecules for the analysis of Brønsted and Lewis acidity, respectively. The main results are shown in Table 2 and Fig. S2–S3 (SI). The Table shows that strong BAS form after the TEA grafting to SiO<sub>2</sub>. Amount of BAS increases until it reaches 12 wt% and then it tends to decrease. Note that strength of BAS also decreases. The existence of BAS is related to the appearance

**Table 2** Brønsted and Lewis acidity of Al-SiO<sub>2</sub> materials determined by FTIR spectroscopy using pyridine and CO as a probe molecules

	Brønsted acid sites <sup>a</sup>		Lewis acid sites <sup>b</sup>		
	N <sub>BAS</sub> (μmol/g)	PA (kJ/mol)	N <sub>Strong</sub> (μmol/g)	N <sub>Medium</sub> (μmol/g)	N <sub>Weak</sub> (μmol/g)
SiO <sub>2</sub>	–	1390	–	15	–
1%Al-SiO <sub>2</sub>	0.5	1190	10	25	60
4%Al-SiO <sub>2</sub>	7.1	1130	50	30	180
6%Al-SiO <sub>2</sub>	14.8	1130	40	35	200
12%Al-SiO <sub>2</sub>	14.5	1130	30	40	300
18%Al-SiO <sub>2</sub>	9.5	1210	30	50	350
γ-Al <sub>2</sub> O <sub>3</sub> [27]	0	0	40	200	520

<sup>a</sup>The number of BAS was estimated from the intensity of the stretching vibration band of pyridinium ions with a maximum at 1540 cm<sup>-1</sup>

<sup>b</sup>The concentration of LAS was estimated from the integral intensity of CO bands for strong strength LAS (2228 cm<sup>-1</sup>); medium strength LAS (2210–2215 cm<sup>-1</sup>) and weak strength of LAS (2180–2200 cm<sup>-1</sup>)

of  groups. Amount of these groups decreases with increasing Al content due to the blocking –Si–OH groups by Al<sub>2</sub>O<sub>3</sub> oligomeric particles. The surface acidity also decreases with the increasing amount of aluminum in Al-SiO<sub>2</sub>. In general, the total amount of BAS is very small in comparison with that of LAS.

On the contrary, the total amount of LAS is growing steadily with increasing amount of Al in the sample (Table 2). According to FTIR spectroscopy, three types of LAS, characterized by bands at 2228 (strong LAS), 2210–2215 (medium LAS), and 2180–2200 cm<sup>-1</sup> (weak LAS), were present in the Al-SiO<sub>2</sub> spectra [28]. Most authors [23, 29, 30] suggest that the surface Lewis acid sites of Al<sub>2</sub>O<sub>3</sub> are formed by electron-acceptor sites represented by coordinatively unsaturated aluminum cations, which may be pentacoordinated (i.e., octahedral with one missing ligand and hence one free coordination site), tetraordinated (normal tetrahedral sites that can expand their coordination or octahedral with two free coordination sites) and trigonal or tricoordinated (octahedral with three free coordination sites or tetrahedral with one free coordination site). The strongest Lewis sites on Al<sub>2</sub>O<sub>3</sub> are formed by tricoordinated Al<sup>3+</sup> ions, while medium and weak strength LAS are formed by tetra- and pentacoordinated Al<sup>3+</sup> ions, respectively. The distribution of LAS in Al-SiO<sub>2</sub> samples is given in Table 2. As can be seen from these data, the Lewis acidity rises with increasing Al content. The rising Al content from 1 to 12 wt% the amount of weak LAS rises from 60 to 350 μmol/g, while the amount of medium and strong LAS changes not so strongly and is in the range of 70–80 μmol/g. Early, effect of Al content on surface acidity was demonstrated for Al-MCM-41 synthesized by grafting method [21]. According to NH<sub>3</sub>-TPD, Al-MCM-41 materials have moderate acidity. The total amount of acid sites rise with increase in the Al incorporation into the framework of the materials due to the acid sites with weak and medium strength.



## Catalytic properties of Al-SiO<sub>2</sub> systems

Catalytic properties of Al-SiO<sub>2</sub> samples in the isomerization of PO to CA were investigated in dichloroethane at 303 K. The reaction in the presence of Al-SiO<sub>2</sub> samples was heterogeneous and that it was investigated by a special test. After 30 min of reaction the 18%Al-SiO<sub>2</sub> sample was filtered off via membrane filter. Then, the filtrate was stirred at 303 K for 30 min (Table 3, runs 7–8). Conversion of PO was not observed after removal of the catalyst from the reaction mixture. The main results are shown in Table 3. According to the experimental data, CA was the main product with 48–72% selectivity at 65–80% conversion of 0.25 mmol PO for 30 min. Some by-products were also formed in addition to campholenic aldehyde (CA) during  $\alpha$ -pinene oxide isomerization. There are fencholenic aldehyde (FA), *trans*-carveol, pinocarveol, pinocamphone, *trans*-sobrerol etc. (Scheme 1). The FA (3–5%) is structural isomer of CA and its mechanism of formation is similar to that of CA. The opening of the epoxide ring of  $\alpha$ -pinene oxide over acid sites leads to the formation of *trans*-carveol, pinocamphone and pinocarveol. The appearance of *trans*-sobrerol in reaction mixture can be explained by the reaction of *trans*-carveol with water that is presence of a small amount (0.1 wt%) in dichloroethane.

As our experimental evidence shows (Table 3, runs 1–6 and 8), the Al content affects the catalytic activity of the Al-SiO<sub>2</sub> samples. The conversion of PO increases with increasing the Al content up to 4 wt% Al, and then does not change, when Al content is in the range of 4–12 wt%. Conversion of PO dramatically decreases in the

**Table 3** Isomerization of PO in the presence of Al-containing materials

Run	Samples	PO conversion (%)	Selectivity, (%)				
			(CA)	(FA)	( <i>trans</i> -carv)	( <i>trans</i> -sobr)	Other <sup>a</sup>
1	SiO <sub>2</sub>	3	50	6	10	6	28
2	0.5%Al-SiO <sub>2</sub>	31	52	6	14	11	17
3	1%Al-SiO <sub>2</sub>	50	61	5	14	9	11
4	4%Al-SiO <sub>2</sub>	75	68	3	14	8	7
5	6%Al-SiO <sub>2</sub>	76	65	3	16	7	9
6	12%Al-SiO <sub>2</sub>	80	72	2	15	8	3
7	18%Al-SiO <sub>2</sub>	65	48	3	16	9	24
8 <sup>b</sup>	18%Al-SiO <sub>2</sub>	66	48	3	16	8	25
9	Al <sub>2</sub> O <sub>3</sub>	43	50	2	17	11	20
10	Fe <sub>3</sub> O <sub>4</sub>	47	34	2	20	13	31
11	SiO <sub>2</sub> /Fe <sub>3</sub> O <sub>4</sub>	52	44	3	18	11	24
12	4%Al-SiO <sub>2</sub> /Fe <sub>3</sub> O <sub>4</sub>	60	51	3	16	8	22
13	12%Al-SiO <sub>2</sub> /Fe <sub>3</sub> O <sub>4</sub>	65	63	3	16	9	9
14	18%Al-SiO <sub>2</sub> /Fe <sub>3</sub> O <sub>4</sub>	65	47	4	15	11	23
15 <sup>b</sup>	18%Al-SiO <sub>2</sub> /Fe <sub>3</sub> O <sub>4</sub>	66	48	4	16	11	21

Experimental condition: 0.25 mmol PO in 2 mL dichloroethane, 5 mg catalyst, 303 K, 30 min

<sup>a</sup>Other by-products were pinocarveol, isopinocampheol, isopinocampnone and fencholenic aldehyde

<sup>b</sup>Catalyst was filtered off after 30 min of reaction and the filtrate was stirred at 303 K for 30 min

next increase in Al content (Table 3, run 7). Conversion of PO was about 43% in the presence of  $\text{Al}_2\text{O}$  (Table 3, run 9). Selectivity towards CA also depends on the Al content. The increasing Al from 0.5 to 12 wt% leads to the change in selectivity from 52 to 72%. In the presence of  $\text{Al}_2\text{O}_3$  selectivity towards CA was 50% (Table 3, run 9).

Several factors account for these correlations. First of all, isomer selectivity depends on the Al content in Al-SiO<sub>2</sub> (Table 1). These data agree with Refs. [14, 31]. Thus, Arate and Tanabe [14] demonstrated that in the presence of  $\text{Al}_2\text{O}_3$  and  $\text{Al}_2\text{O}_3\text{-SiO}_2$  ( $\text{Al}_2\text{O}_3$ —15 wt%) the selectivities towards CA were 37–46% and 70%, respectively. Therefore our results are in line with other studies.

Moreover, nature of active site also can affect the reaction rate and selectivity of reaction. The LAS promote the formation of CA, whereas BAS mainly favour the generation of *trans*-carveol [7]. Indeed, a larger amount of LAS in comparison with that of BAS (Table 2) is one of the reasons for the high isomer selectivity towards CA (Table 3). The strength of LAS also affects the distribution products. We can assume that activation of oxygen atom of epoxy-group of PO preferably takes place on the centers with medium and strong strength. LAS with weak strength also can take part in the reaction process, but their contribution is likely negligible. Correlations between the amount of medium and strong LAS and selectivity towards CA confirm this assertion (Fig. S3, SI). Note that the strength of LAS is one of the main parameters which can affect the reaction rate in the presence of Al-SiO<sub>2</sub>. As shown in Fig. S3 (SI), the increase in the strength of LAS from 1190 kJ/mol (1%Al-SiO<sub>2</sub>) to 1130 kJ/mol (4–12%Al-SiO<sub>2</sub>) leads to increasing PO from 50 to 75–80%. The low conversion of PO (65%) in the presence of 18%Al-SiO<sub>2</sub> can account for the low strength of LAS (1210 kJ/mol).

The dramatically decreasing selectivity of CA in the presence of 18%Al-SiO<sub>2</sub> leads us to think that one of the important parameters for activity and selectivity of the reaction also is the oligomeric state of  $\text{Al}_2\text{O}_3$  species on the surface of Al-SiO<sub>2</sub>. The changing the oligomeric state with variation of Al content was qualitatively estimated from the analysis of changing of the yield of CA based on  $S_{\text{BET}}$  ( $Y_{\text{CA}}/S_{\text{BET}}$ ,  $\mu\text{mol}/(\text{m}^2 \text{g}^{-1})$ ):

$$4\% \text{Al} - \text{SiO}_2(0.57) > 6\% \text{Al} - \text{SiO}_2(0.46) \sim 12\% \text{Al} - \text{SiO}_2(0.48) > 18\% \text{Al} - \text{SiO}_2(0.35)$$

The decreasing this value is related to the increasing amount of oligomeric  $\text{Al}_2\text{O}_3$  species. The effect of the oligomeric state of the metal oxide particles on the efficiency of the catalyst is not a unique in catalysis and was demonstrated for isomerization of PO to CA in the presence of iron modified zeolites (beta and ZSM-5), MCM-41, SiO<sub>2</sub> and  $\text{Al}_2\text{O}_3$  [32], Fe-VSB-5 and Fe-SBA-3 [33].

The changes in textural properties with increasing Al content in Al-SiO<sub>2</sub> also should be taken into account. Conversion of PO and selectivity towards CA correlate with specific surface area ( $S_{\text{BET}}$ ) and porosity of samples ( $V_{\mu}/V_{\Sigma}$ ) (Table 1). The reaction rate and selectivity rise with increasing  $S_{\text{BET}}$  and  $V_{\mu}/V_{\Sigma}$  (Table 1, 1%Al-SiO<sub>2</sub>–12%Al-SiO<sub>2</sub> samples). Catalytic properties of 18%Al-SiO<sub>2</sub>, however, are being fall dramatically by the decreasing  $S_{\text{BET}}$  and  $V_{\mu}/V_{\Sigma}$ . Thus, we can say that catalytic properties of Al-SiO<sub>2</sub> materials are tunable by the variation of micro-

mesoporous structure. Note that this phenomenon was demonstrated by Ravindra et al. [8] for Al-MSU-SFAU (Si/Al 70), which was synthesized from nanoclustered zeolite Y seeds as framework precursors, and possessed a mesoporous structure with the walls having microporosity. In the presence of Al-MSU-SFAU the selectivity towards CA was 86% at 54% conversion of PO. The high selectivity was explained by the short length of channels that did not allow further reactions to other isomers occur.

### Synthesis and investigation of magnetically Al-SiO<sub>2</sub>/Fe<sub>3</sub>O<sub>4</sub> systems

Fe<sub>3</sub>O<sub>4</sub> magnetic nanoparticles were used as a support for the synthesis of the Al-SiO<sub>2</sub>/Fe<sub>3</sub>O<sub>4</sub> nanocomposite catalysts with controllable reactivity and magnetic recyclability. Synthesis of Al-SiO<sub>2</sub>/Fe<sub>3</sub>O<sub>4</sub> samples was based on the Al-SiO<sub>2</sub> synthesis strategy and had three stages (Scheme 2): (i) synthesis of magnetite Fe<sub>3</sub>O<sub>4</sub> nanoparticles, (ii) coating magnetic Fe<sub>3</sub>O<sub>4</sub> particles with silica, and (iii) grafting of Al-organic compounds to silica and the following calcination at 973 K. In general, synthesis of Al-SiO<sub>2</sub>/Fe<sub>3</sub>O<sub>4</sub> materials was based on our knowledge of the synthesis of Al-SiO<sub>2</sub> materials under which Al content on the surface of Al-SiO<sub>2</sub> affects its catalytic properties. At this point, we synthesized the corresponding Al-SiO<sub>2</sub>/Fe<sub>3</sub>O<sub>4</sub> samples with 4, 12 and 18 wt% Al content.

The morphology and size distribution of the particles were examined by high-resolution transmission electron microscopy. Fig. 2 shows the HR-TEM image of 12%Al-SiO<sub>2</sub>/Fe<sub>3</sub>O<sub>4</sub> sample. It can be seen that the size of magnetite Fe<sub>3</sub>O<sub>4</sub> nanoparticles has uniform distribution with an average dimension of 8–15 nm. The surface of the Fe<sub>3</sub>O<sub>4</sub> nanoparticles is coated with silica layer. The thickness of the layer is about 5 nm thick. The following coating of Al<sub>2</sub>O<sub>3</sub> by post-synthesis grafting method leads to form Al species with an island structure (Fig. 2c (C)).

The catalytic properties of the Al-SiO<sub>2</sub>/Fe<sub>3</sub>O<sub>4</sub> samples were investigated in the isomerization of PO to CA. Experimental conditions were similar to that in the presence of Al-SiO<sub>2</sub>. The main results are presented in Table 3. In this case the main products also were CA, *trans*-carv and *trans*-sobr. Reaction did not proceed without

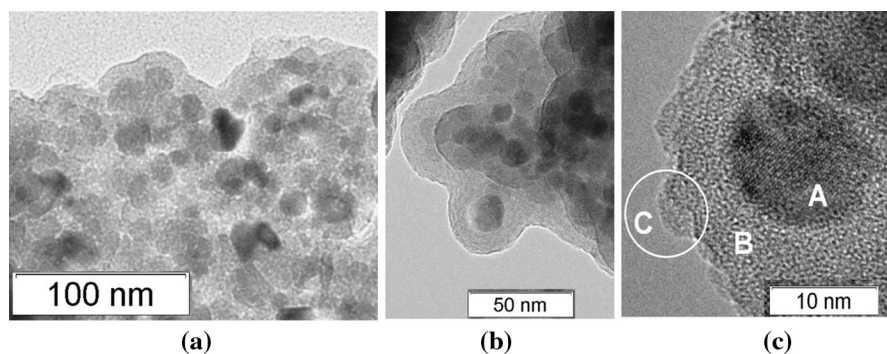


**Fig. 2** HR-TEM image of 12% Al-SiO<sub>2</sub>/Fe<sub>3</sub>O<sub>4</sub>. In c (A) Fe<sub>3</sub>O<sub>4</sub>, (B) layer of SiO<sub>2</sub> and (C) phase of SiO<sub>2</sub> enriched by Al<sub>2</sub>O<sub>3</sub>

catalyst, because after removal of the catalyst conversion of PO and distribution of products did not change (Table 3, runs 14–15). As expected, reaction rate and selectivity depended on the Al content in Al-SiO<sub>2</sub>/Fe<sub>3</sub>O<sub>4</sub>. The optimal Al content was 12 wt%. However, in contrast to 12%Al-SiO<sub>2</sub>, 12%Al-SiO<sub>2</sub>/Fe<sub>3</sub>O<sub>4</sub> gave lower conversion of PO and selectivity towards CA, readily accounted for by differences in textural properties and Al aggregation state (Table 3, runs 6 and 13).

Several reasons might be adduced to explain the difference in catalytic properties of 12%Al-SiO<sub>2</sub> and 12%Al-SiO<sub>2</sub>/Fe<sub>3</sub>O<sub>4</sub>. First of all, it may be related to the differing textural properties (Table 1). 12%Al-SiO<sub>2</sub> possesses larger specific surface area, total pore volume and micropore volume in compared with 12%Al-SiO<sub>2</sub>/Fe<sub>3</sub>O<sub>4</sub>. At the same time, pore diameter ( $D_{\text{pore}}$ ) and  $V_{\mu}/V_{\Sigma}$  value are larger for 12%Al-SiO<sub>2</sub>/Fe<sub>3</sub>O<sub>4</sub>. The largest  $V_{\mu}/V_{\Sigma}$  can provoke diffusion problems and, therefore, to decrease reaction rate, whereas the largest diameter of pore can affect the spatial arrangement and configuration of intermediates and, thereby determine the isomer selectivity. Other reason can be related to the impact of Fe on catalytic properties of Al-SiO<sub>2</sub>/Fe<sub>3</sub>O<sub>4</sub> samples as confirmed by the catalytic test in the presence of SiO<sub>2</sub>/Fe<sub>3</sub>O<sub>4</sub> (Table 3, run 10).

### The catalytic potential of Al-SiO<sub>2</sub> and Al-SiO<sub>2</sub>/Fe<sub>3</sub>O<sub>4</sub> materials

First of all, it is interesting to compare the catalytic behavior of Al-SiO<sub>2</sub> with that of Fe-VSB-5 and Fe-containing mesoporous silica materials (Fe-MMM-2) [33]. Within the Fig. S4 (SI) is contained correlations between surface acidity and reaction rate and selectivity towards CA for these materials. As can be seen from these correlations, selectivity towards CA rises with increasing amount of LAS in Al-SiO<sub>2</sub> that is similar to Fe-VSB-5. At the same time, the opposite trend is observed with respect to Fe-MMM-2 that is related to a large oligomeric iron oxide species in framework of solid. Therefore, all these results indicate that the high selectivity is a result of well-dispersed Lewis acid sites in a matrix.

Furthermore, we compared efficiency of these samples with that of Al- and Fe-containing materials reported in literature. Because experimental conditions were different, productivity of catalysts was calculated using Eq. 2:

$$\text{Productivity} = \frac{\text{Amount of CA}}{\text{Amount of catalyst} \cdot \text{Reaction time}} = \frac{\text{mmol}}{\text{g} \cdot \text{h}} \quad (2)$$

As is clear from Table S1 (SI) (runs 1–3), in the presence of 12%Al-SiO<sub>2</sub> selectivity towards CA is comparable with that in the presence of Al<sub>2</sub>O<sub>3</sub>-SiO<sub>2</sub> commercial and Al<sub>2</sub>O<sub>3</sub> sulfated systems. In general, productivity of 12%Al-SiO<sub>2</sub> is higher in comparison with other samples. However, in spite of low productivity of Al-MSU (Si/Al=70) selectivity towards CA is higher (86%) in comparison with 12%Al-SiO<sub>2</sub> (72%) (Table S1 (SI), runs 1 and 7). The comparison of catalytic properties of 12%Al-SiO<sub>2</sub>/Fe<sub>3</sub>O<sub>4</sub> with that of Fe-SiO<sub>2</sub> and Fe-Al<sub>2</sub>O<sub>3</sub> prepared by the impregnation method [32] points the advantage of post-synthesis grafting method (Table S1 (SI), runs 9–14).

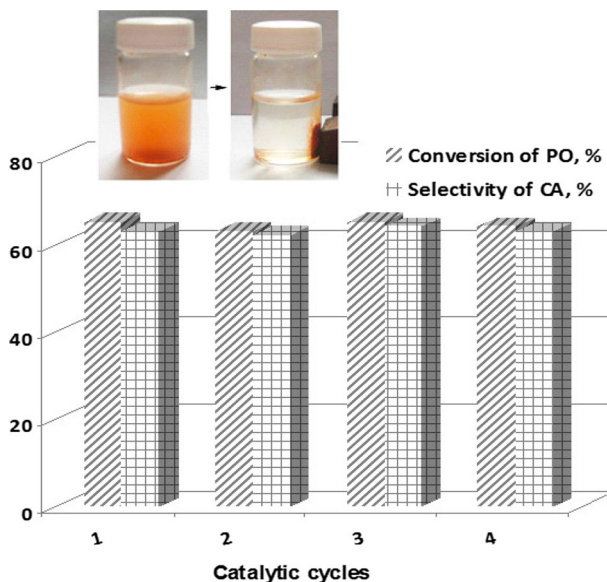


**Fig. 3.** 12% Al-SiO<sub>2</sub>/Fe<sub>3</sub>O<sub>4</sub> recycling during the isomerization of PO. The amount of the reactants was corrected based on reaction conditions (Experimental conditions: 0.25 mmol of PO in 2 mL dichloroethane, 5 mg of catalyst, 303 K, 30 min)

Against this background, the central question also was to investigate the reusability and the recycling use of the 12%Al-SiO<sub>2</sub>/Fe<sub>3</sub>O<sub>4</sub> catalyst. Taking into account the magnetic response of Al-SiO<sub>2</sub>/Fe<sub>3</sub>O<sub>4</sub> materials, after each catalytic experiment, the used 12%Al-SiO<sub>2</sub>/Fe<sub>3</sub>O<sub>4</sub> catalyst was separated from the reaction mixture by the external permanent magnet (Fig. 3). Then, the catalyst was washed by dichloroethane and used in the next cycle. According to experimental data, 12%Al-SiO<sub>2</sub>/Fe<sub>3</sub>O<sub>4</sub> can be used repeatedly without significant loss of catalytic activity during at least four catalytic cycles (Fig. 3).

## Conclusions

Herein, we demonstrated synthesis of the Al-SiO<sub>2</sub> and magnetically recyclable Al-SiO<sub>2</sub>/Fe<sub>3</sub>O<sub>4</sub> samples with 0.5–18 wt% Al content. Synthesis of samples was based on the (i) grafting of triethylaluminum to silica or coating of magnetic Fe<sub>3</sub>O<sub>4</sub> particles by silica under anhydrous conditions and (ii) the following calcination at 973 K. Samples were characterized by various techniques including elemental and N<sub>2</sub>-adsorption/desorption analyses, transmission electron microscopy (TEM), and Fourier transform infrared spectroscopy (FTIR) using CO and pyridine as probe molecules. It was found that LAS and BAS formed after modification of SiO<sub>2</sub> by triethylaluminum. The strength and amount of these sites depended on the Al content. The aluminum monolayer coverage by triethylaluminum was found to be about 5–6 wt%. The next increase in Al content led to the polylayer cover of the SiO<sub>2</sub> surface

(i.e. the formation of  $\text{Al}_2\text{O}_3$  agglomerates). The 12%Al-SiO<sub>2</sub> sample had optimal acidity.

The catalytic properties of the Al-SiO<sub>2</sub> and Al-SiO<sub>2</sub>/Fe<sub>3</sub>O<sub>4</sub> samples were investigated in the isomerization of PO to CA. The reaction rate and isomer selectivity towards CA were found to dramatically decrease when Al content was more than 12 wt%. This phenomenon was related to the changing of textural and acid–base properties. Investigation of 12%Al-SiO<sub>2</sub>/Fe<sub>3</sub>O<sub>4</sub> stability pointed that sample can be used repeatedly without significant loss of catalytic activity during at least four catalytic cycles.

**Acknowledgements** This work was conducted within the framework of the budget Project AAAA-A17-117041710082–8 for Boreskov Institute of Catalysis.

### Compliance with ethical standards

**Conflict of interest** There are no conflicts of interest to declare.

### References

1. Erman WE (1985) Chemistry of the monoterpenes, An encyclopedic handbook. Marcel Dekker, New York
2. Volcho KP, Salakhutdinov NF (2008) Transformations of terpenoids on acidic clays. *Mini-Rev Org Chem* 5:345–354. <https://doi.org/10.2174/157019308786242151>
3. Ohloff G, Winter B, Fehr C, Muller PM, Lamparsky D (eds) (1991) *Perfumes, art, science and technology*. Elsevier, New York, pp 287–330
4. da Silva Rocha KA, Hoehne JL, Gusevskaya EV (2008) Phosphotungstic acid as a versatile catalyst for the synthesis of fragrance compounds by  $\alpha$ -pinene oxide isomerization: solvent induced chemoselectivity. *Chemistry* 14:6166–6172. <https://doi.org/10.1002/chem.200800184>
5. Lewis JB, Hedrick GW (1965) Reaction of  $\alpha$ -pinene oxide with zinc bromide and rearrangement of 2,2,3-trimethyl-3-cyclopentenep derived there from. *J Org Chem* 30:4271–4275. <https://doi.org/10.1021/jo01023a064>
6. Kaminska J, Schwegler MA, Hoenfnagel AJ, van Bekkum H (1992) The isomerisation of  $\alpha$ -pinene oxide with Brønsted and Lewis acids. *Recl Trav Chim Pays-Bas* 111:432–437. <https://doi.org/10.1002/recl.19921111004>
7. Holderich WF, Roseler J, Heitmann G, Liebens AT (1997) The use of zeolites in the synthesis of fine and intermediate chemicals. *Catal Today* 37:353–366. [https://doi.org/10.1016/S0920-5861\(97\)81094-2](https://doi.org/10.1016/S0920-5861(97)81094-2)
8. Ravindra DB, Nie YT, Jaenicke S, Chuah GK (2004) Isomerisation of  $\alpha$ -pinene oxide over B<sub>2</sub>O<sub>3</sub>/SiO<sub>2</sub> and Al-MSU catalysts. *Catal Today* 96:147–153. <https://doi.org/10.1016/j.cattod.2004.06.117>
9. Kunkeler PJ, van der Waal JC, Bremmer J, Zuurdeeg BJ, Downing RS, van Bekkum H (1998) Application of zeolite titanium Beta in the rearrangement of  $\alpha$ -pinene oxide to campholenic aldehyde. *Catal Lett* 53:135–138. <https://doi.org/10.1023/A:1019049704709>
10. Jarry B, Launay F, Nogier JP, Bonardet JL (2007) Comparative study of the catalytic activity of Al-SBA-15 and Ga-SBA-15 materials in  $\alpha$ -pinene isomerisation and oxidative cleavage of epoxides. *Stud. Surf. Sci. Catal.* 165:791–794
11. Liebens AT, Mahaim C, Holderich WF (1997) Selective isomerization of  $\alpha$ -pinene oxide with heterogeneous catalysts. *Stud Surf Sci Catal* 108:587–594. [https://doi.org/10.1016/S0167-2991\(97\)80954-8](https://doi.org/10.1016/S0167-2991(97)80954-8)

12. Panadero MP, Vely A (2019) Readily available Ti-beta as an efficient catalyst for greener and sustainable production of campholenic aldehyde. *Catal Sci Technol* 9:1293–4303. <https://doi.org/10.1039/c9cy00957d>
13. Štekrova M, Kubů M, Shamzhy M, Musilova Z, Cejka J (2018)  $\alpha$ -Pinene oxide isomerization: role of zeolite structure and acidity in the selective synthesis of campholenic aldehyde. *Catal Sci Technol* 8:2488–2501. <https://doi.org/10.1039/c8cy00371h>
14. Arata K, Tanabe K (1979) Isomerization of  $\alpha$ -pinene oxide over solid acids and bases. *Chem Lett*. <https://doi.org/10.1246/cl.1979.1017>
15. Ravasio N, Zaccheria F, Guidotti M, Psaro R (2004) Mono- and bifunctional heterogeneous catalytic transformation of terpenes and terpenoids. *Top Catal* 27:157–168. <https://doi.org/10.1023/B:TOCA.0000013550.28170.6a>
16. Polshettiwar V, Luque R, Fihri A, Zhu H, Bouhrara M, Basset J-M (2011) Magnetically recoverable nanocatalysts. *Chem Rev* 111:3036–3075. <https://doi.org/10.1021/cr100230z>
17. Liu J, Qiao SZ, Hu QH, Lu GQ (2011) Magnetic nanocomposites with mesoporous structures: synthesis and applications. *Small* 7:425–443. <https://doi.org/10.1002/sml.201001402>
18. Shylesh S, Schenemann V, Thiel WR (2010) Magnetically separable nanocatalysts: bridges between homogeneous and heterogeneous catalysis. *Angew Chem Int Ed* 49:3428–3459. <https://doi.org/10.1002/anie.200905684>
19. Baig RBN, Varma RS (2013) Magnetically retrievable catalysts for organic synthesis. *Chem Commun* 49:752–770. <https://doi.org/10.1039/C2CC35663E>
20. Iengo P, Di Serio M, Sorrentino A, Solinas V, Santacesaria E (1998) Preparation and properties of new acid catalysts obtained by grafting alkoxides and derivatives on the most common supports: note I—grafting aluminium and zirconium alkoxides and related sulphates on silica. *Appl Catal A* 167:85–101. [https://doi.org/10.1016/S0926-860X\(97\)00303-7](https://doi.org/10.1016/S0926-860X(97)00303-7)
21. Jana SK, Kugita T, Namba S (2004) Aluminum-grafted MCM-41 molecular sieve: an active catalyst for bisphenol F synthesis process. *Appl Catal A* 266:245–250. <https://doi.org/10.1016/j.apcata.2004.02.013>
22. Kirillov VL, Balaev DA, Semenov SV, Shaikhutdinov KA, Martyanov ON (2014) Size control in the formation of magnetite nanoparticles in the presence of citrate ions. *Mater Chem Phys* 145:75–81. <https://doi.org/10.1016/j.matchemphys.2014.01.036>
23. Panchenko VN, Danilova IG, Zakharov VA, Semikolenova NV, Paukshtis EA (2017) Effect of the acid-base properties of the support on the catalytic activity of ethylene polymerization using supported catalysts composed of  $Cp_2ZrX_2$  ( $X = Cl, Me$ ) and  $Al_2O_3(F)$ . *Reac Kinet Mech Cat* 122:275–287. <https://doi.org/10.1007/s1144-017-1215-x>
24. Caillot M, Chaumonnot A, Digne M, van Bokhoven JA (2014) Creation of Brønsted acidity by grafting aluminum isopropoxide on silica under controlled conditions: determination of the number of Brønsted sites and their turnover frequency for m-xylene isomerization. *Chem Catal Chem* 6:2–841. <https://doi.org/10.1002/cctc.201300824>
25. Leydier F, Chizallet C, Chaumonnot A, Digne M, Soyer E, Quoineaud AA, Costa D, Raybaud P (2011) Brønsted acidity of amorphous silica-alumina: the molecular rules of proton transfer. *J Catal* 284:215–229. <https://doi.org/10.1016/j.jcat.2011.08.015>
26. Zaki MI, Knözinger H (1987) Carbon monoxide: a low temperature infrared probe for the characterization of hydroxyl group properties on metal oxide surfaces. *Mater Chem Phys* 17:201–221. [https://doi.org/10.1016/0254-0584\(87\)90056-3](https://doi.org/10.1016/0254-0584(87)90056-3)
27. Zhuravlev LT (2000) The surface chemistry of amorphous silica. *Zhuravlev Model Colloids Surf A* 173:1–38. [https://doi.org/10.1016/S0927-7757\(00\)00556-2](https://doi.org/10.1016/S0927-7757(00)00556-2)
28. Glazneva TS, Kotsarenko NS, Paukshtis EA (2008) Surface acidity and basicity of oxide catalysts: From aqueous suspensions to in situ measurements. *Kinet Catal* 49:859–867. <https://doi.org/10.1134/S0023158408060104>
29. Busca G (2014) Structural, surface, and catalytic properties of aluminas. *Adv Catal* 57:319–404. <https://doi.org/10.1016/B978-0-12-800127-1.00003-5>
30. Belskaya OB, Danilova IG, Kazakov MO, Mironenko RM, Lavrenov AV, Likholobov VA (2012). FTIR spectroscopy of adsorbed probe molecules for analyzing the surface properties of supported Pt (Pd) catalysts, infrared spectroscopy—materials science, engineering and technology, Prof. Theophanides Theophile (ed.), pp 149–178. ISBN: 978-953-51-0537-4
31. Nigam IC, Levi L (1968) Essential oils and their constituents. XLII. Isomerization of epoxides on active alumina. *Can J Chem* 46:1944–1947. <https://doi.org/10.1139/v68-321>

32. Stekrova M, Kumar N, Aho A, Sinev I, Grunert W, Dahl J, Roine J, Arzhumanov AS, Maki-Arvela P, Murzin DYu (2014) Isomerization of alfa-pinene oxide using Fe-supported catalysts: Selective synthesis of campholenic aldehyde. *Appl Catal A* 470:162–176. <https://doi.org/10.1016/j.apcata.2013.10.044>
33. Timofeeva MN, Panchenko VN, Hasan Z, Khan NA, Mel'gunov MS, Abel AA, Matrosova MM, Volcho KP, Jhung SH (2014) Effect of iron content on selectivity in isomerization of  $\alpha$ -pinene oxide to campholenic aldehyde over Fe-MMM-2 and Fe-VSB-5. *Appl Catal A* 469:427–433. <https://doi.org/10.1016/j.apcata.2013.10.016>

**Publisher's Note** Springer Nature remains neutral with regard to jurisdictional claims in published maps and institutional affiliations.